



Published in final edited form as:

Cancer Res. 2009 December 1; 69(23): 8932–8940. doi:10.1158/0008-5472.CAN-08-3873.

Human Bone Marrow-Derived Mesenchymal Stem Cells for Intravascular Delivery of Oncolytic Adenovirus Delta-24-RGD to Human Gliomas

Raymund L. Yong^{1,4,5}, Naoki Shinojima^{1,4}, Juan Fueyo^{2,4}, Joy Gumin^{1,4}, Giacomo G. Vecil^{1,4}, Frank C. Marini³, Oliver Bogler^{1,4}, Michael Andreeff³, and Frederick F. Lang^{1,4}

¹Department of Neurosurgery, The University of Texas M. D. Anderson Cancer Center, , 1515 Holcombe Boulevard, Houston, Texas 77030, USA

²Department of Neuro-oncology, The University of Texas M. D. Anderson Cancer Center, , 1515 Holcombe Boulevard, Houston, Texas 77030, USA

³Department of Stem Cell Transplantation, The University of Texas M. D. Anderson Cancer Center, , 1515 Holcombe Boulevard, Houston, Texas 77030, USA

⁴Brain Tumor Center, The University of Texas M. D. Anderson Cancer Center, , 1515 Holcombe Boulevard, Houston, Texas 77030, USA

⁵Division of Neurosurgery, Department of Surgery, The University of British Columbia, 3100 – 910 West 10th Avenue, Vancouver, British Columbia V5Z 4E3, Canada.

Abstract

Delta-24-RGD is an infectivity-augmented, conditionally-replicative oncolytic adenovirus with significant antiglioma effects. Although intratumoral delivery of Delta-24-RGD may be effective, intravascular delivery would improve successful application in humans. Due to their tumor tropic properties, we hypothesized that human mesenchymal stem cells (hMSCs) could be harnessed as intravascular delivery vehicles of Delta-24-RGD to human gliomas. To assess cellular events, GFP-labeled hMSCs carrying Delta-24-RGD (hMSCs-Delta24) were injected into the carotid artery of mice harboring orthotopic U87MG or U251-V121 xenografts and brain sections were analyzed by immunofluorescence for GFP and viral proteins (E1A and hexon) at increasing times. hMSCs-Delta24 selectively localized to glioma xenografts and released Delta-24-RGD, which subsequently infected glioma cells. To determine efficacy, mice were implanted with luciferase-labeled glioma xenografts, treated with hMSCs-Delta24 or controls and imaged weekly by bioluminescence imaging (BLI). Analysis of tumor size by BLI demonstrated inhibition of glioma growth and eradication of tumors in hMSCs-Delta24-treated animals compared with controls ($P < 0.0001$). There was an increase in median survival from 42 days in controls to 75.5 days in hMSC-Delta-24-treated animals ($P < 0.0001$) and an increase in survival beyond 80 days from 0% to 37.5%, respectively. We conclude that intra-arterially delivered hMSCs-Delta24 selectively localize to human gliomas, and are capable of delivering and releasing Delta-24-RGD into the tumor, resulting in improved survival and tumor eradication in subsets of mice.

Introduction

Current treatments for glioblastoma, the most common adult malignant brain tumor, result in a median survival of only 14 months (1). However, recent evidence has demonstrated that Delta-24-RGD, a tumor-selective, replication-competent adenovirus with augmented cellular infectivity, may be effective against this fatal disease (2,3). Because it contains a mutant viral E1A gene, Delta-24-RGD selectively replicates in and lyses tumor cells in which the retinoblastoma protein (Rb) is inactivated. Delta-24-RGD's augmented infectivity is due to an insertion of an RGD-motif in the fiber knob, allowing for integrin-mediated infection, independent of cocksackie-adenovirus receptors (CAR) (4,5), which are minimally expressed in gliomas. In an orthotopic model of human gliomas, intratumoral injection of Delta-24-RGD resulted in a significantly longer survival than controls (3).

Despite success in preclinical models, human gliomas in patients are heterogeneous, containing multiple barriers to viral spread that represent hurdles for successful virus-mediated tumor eradication after intratumoral injection (6-8). Intravascular delivery may overcome these barriers because it can produce widespread initial viral distribution in the tumor and repeat dosing is possible. Unfortunately, intravascular administration of adenovirus is limited by liver toxicity and neutralizing antibodies (8-10).

Recent evidence has demonstrated that human bone marrow-derived mesenchymal stem cells (hMSCs) are useful delivery vehicles for brain tumor therapy (11). hMSCs are well-suited for clinical applications because they are easily obtained from patients, their procurement poses no ethical concerns, and autologous transplantation is possible (12,13). We have shown that hMSCs selectively localize to human gliomas after intravascular administration, and they can deliver anti-glioma agents to orthotopic models of the disease (11,14). Their capacity to localize to gliomas may reflect an intrinsic ability of MSCs to home to most solid tumors (15-18).

Previous work using hMSCs to deliver oncolytic adenoviruses to tumors has met with some success (19-21). However, these studies have provided limited information about the cellular events underlying the intravascular delivery of oncolytic viruses via hMSCs. The effects of Delta-24-RGD on the tropism of hMSCs for gliomas after intravascular delivery remain unknown. Moreover, it is unclear whether hMSCs loaded with Delta-24-RGD are capable of lysing and releasing the virus once within gliomas. Because hMSCs express normal Rb, *a priori* one would not expect Delta-24-RGD to replicate in hMSCs. However, there may be a window for viral replication during stem cell self-renewal during which Rb is inactivated. Lastly, no study has demonstrated improvements in survival when MSCs are used to deliver viral therapies to gliomas. Although one report suggests that hMSCs carrying oncolytic viruses can migrate short distances toward brain tumors after juxtatumoral injection, efficacy was not shown, and the feasibility of intravascular delivery was not explored (22). Here, we address these issues and demonstrate for the first time that hMSCs are able to deliver Delta-24-RGD to human gliomas after intravascular injection and that this strategy results in long term survival in animal models of gliomas.

Methods

Mesenchymal stem cells

Male hMSCs were obtained from Lonza (Walkersville, MD). Cells were positive for CD44, CD73, CD90 and CD105 and negative for CD34, CD45, and CD133. Cells were expanded in a °C, 5% CO₂ incubator in α -MEM containing 10% fetal bovine serum (Sigma, MO), 1% 2mM L-glutamine (Invitrogen, NY), and 1% penicillin-streptomycin (Lonza) and were used at passage 5-7.

Tumor cells

Glioblastomas U87MG, LN229 were obtained from ATCC (Manassas, VA). D54 was provided by Darell Bigner (Duke University, NC), and U251 and U251-V121 by WK Alfred Yung (M. D. Anderson). Cells were grown in MEM- α 10% FBS, 1% penicillin-streptomycin. U87MG-GL, containing *Gfp* and luciferase were obtained from T. J.Liu (M. D. Anderson). U87MG-LucNeo, described previously (23,24), were provided by B.S. Carter (MGH, Boston, MA) and grown in U87MG media containing Zeocin 0.5mg/ml (Invitrogen). U87MG-XO karyotype cells were selected from U87MG by cloning single XO cells.

MSC labeling and infection

hMSCs were transduced with *Gfp* using a replication-incompetent Ad5/F35-CMV-GFP (Ad-GFP) (25) (Vector Development Laboratory, Baylor College of Medicine, Houston, TX). Monolayers were treated with 50MOI in 3ml serum-free hMSC-media shaken every 10min at $^{\circ}$ C. After 1hr, hMSC-media containing 10%FBS was added. For infection with Delta-24-RGD 10-100pfu/cell of viral stock solution was added to the 3 ml serum-free media mixture containing Ad5/F35-CMV-GFP.

Cell cycle analysis

3×10^5 hMSCs were cultured in serum-free media for 72 hours to synchronize cells. Cells were infected with Delta-24-RGD at 0 (sham), 10, 50 and 100MOI in serum-free media. At 1 hour, α -MEM containing 10% FBS was added and hMSCs were collected and fixed 24, 48, and 72hrs later. Collected hMSCs were centrifuged and resuspended in 500 μ l PBS. RNase A (Roche Applied Science, IN) was added followed by propidium iodide (100 μ l/ml cells, Roche Applied Science) and analyzed by flow cytometry.

Viral titering

2×10^5 hMSCs were plated for 24hrs then infected with Delta-24-RGD at various multiplicities over 1hr, after which growth media was added. After infection, the media was collected and cells trypsinized and centrifuged. The collected media was added to the pellet and cells were resuspend. Each sample was subjected to 3 freeze-thaw cycles to lyse hMSCs. After centrifugation, the titer in supernatant was determined using the Adeno-X RapidTiter Kit (Clontech Laboratories, CA).

In vitro efficacy testing

Transwell experiments were performed using 0.4 μ m pore plates (Corning Inc., NY). hMSCs infected with various MOIs of Delta-24-RGD were collected, washed, replated in the upper well at 1×10^4 cells/well, and placed over lower wells containing glioma cells (3×10^4 cells/well). After 7 days, viable glioma cells were counted using an automated hemocytometer.

Animals

Male athymic mice (*nu/nu*) (Department of Experimental Radiation Oncology, M.D.Anderson) were manipulated according to institutional approved protocols and anesthetized using 0.25 ml of 10 mg/ml ketamine and 1 mg/ml xylazine cocktail, IP.

Intracranial glioma xenograft implantation

Glioma cells were implanted via cranial guide screws as described previously (26). Mice received 5×10^5 (U87) or 1×10^6 (U251-V121) cells via a Hamilton syringe inserted to a depth of 5 mm. Ten mice were implanted simultaneously using a microinfusion syringe pump (0.5 μ l/min) (Harvard Apparatus, MA) as described previously (11).

Internal carotid artery injection of MSCs

hMSCs were trypsinized, centrifuged (1500 rpm, 5 minutes, x3) and resuspended in hMSC media with 10% FBS at 1×10^6 cells/100 μ l. Injection the right carotid artery was performed as previously described (27), except that a 30g needle was used to inject cells.

Tissue preparation/fixation and immunostaining

Mice were sacrificed by intracardiac perfusion of PBS and 4% paraformaldehyde. Brains were removed, fixed in 10% formalin for 24 hours, embedded in paraffin, and cut (5 μ m-sections). Detection of Delta-24-RGD was performed using mouse anti-hexon (1:100 dilution; Santa Cruz Biotechnology, CA) and rabbit anti-E1A (1:200 dilution; Santa Cruz) antibodies. GFP-labeled hMSCs were detected with rabbit anti-GFP antibodies (1:200 dilution; Santa Cruz). Immunohistochemistry was performed using the ImmPRESS Antibody Kit (Vector Laboratories, CA). Immunofluorescence used biotinylated secondary antibodies and fluorescein- or Texas Red-conjugated avidin (Vector Laboratories).

FISH

Hybridization was performed using dual color subcentromeric-probes for human X or Y chromosomes (Vysis, IL) according to the manufacturer's recommendations.

BLI

Mice were imaged with Xenogen IVIS 200 system (Xenogen Corporation, Alameda, CA), after administering 4mg D-Luciferin, IP. Images were collected using exposure times between 0.1sec and 5mins. BLI were overlaid on grayscale photographic images using Living Image 3.0 software (Xenogen Corp.). Data analysis was based on the total photon flux from a standard-size region of interest.

Statistical Analysis

Cell counts were expressed as means +/- standard deviation. Comparisons were made using 2-way ANOVA. BLI data were analyzed using nonlinear regression based on an exponential growth model and compared using the extra sum-of-squares F-test. Survival curves were compared using the log-rank test. Analyses were performed using GraphPad Prism 5.01.

Results

Delta-24-RGD infection and replication within hMSCs *in vitro*

Because our strategy involves *ex vivo* transduction of hMSCs, we investigated the extent to which Delta-24-RGD is capable of infecting hMSCs. hMSCs express integrins, but lack CAR (28); thus, we compared the infectivity of hMSCs by adenoviral vectors expressing or lacking the RGD-motif, and found increased infectivity Ad-RGD (Supplementary Figure 1A). To verify this result for Delta-24-RGD, we infected hMSCs with Delta-24-RGD containing *Gfp* as a reporter (Delta-24-RGD-GFP). More than 80% of hMSCs expressed GFP after 24 hours (Supplementary Figure 1B) and after 72 hours, nearly all hMSCs exhibited cytopathic effect (Supplementary Figure 1C). Because Delta-24-RGD replicates poorly in cells with normal Rb-pathways (2,3), this result suggests that Rb in hMSCs is inactivated independently of adenoviral E1A when hMSCs spontaneously enter S phase, allowing hMSCs to support the replication of Delta-24-RGD.

hMSCs carrying Delta-24-RGD localize to human gliomas after intracarotid delivery

To determine the extent to which hMSCs carrying Delta-24-RGD are capable of selectively localizing to gliomas after intravascular delivery *in vivo*, U87MG cells (5×10^5) were implanted

into the frontal lobes of nude mice (n=6). One day before delivery hMSCs were transduced with Delta-24-RGD (10 MOI) and Ad-GFP (50 MOI), generating hMSC-Delta24-AdGFP and injected into the right carotid artery (1×10^6 cells/100 μ l media) of mice harboring 7-day-old xenografts. Mice were sacrificed 4 days later (Figure 1). Immunofluorescence staining with anti-GFP antibodies demonstrated hMSCs throughout the tumors (Figure 1A). Virtually no hMSCs were seen elsewhere in the brain. Similar results were obtained using U251-V121 xenografts (Supplementary Figure 2). Sex-mismatched transplant experiments using XO-genotype U87MG xenografts (See Methods) and male (XY) hMSCs confirmed that GFP-positive cells within the xenografts were hMSCs (Figure 1B).

Delta-24-RGD infection of xenografts requires hMSCs

To show that hMSCs are required for Delta-24-RGD to infect gliomas after intravascular delivery, U87MG cells were implanted into the brains of nude mice. After 7 days mice (n=3 per group) were injected with 1×10^6 hMSCs-Delta24 (transduced with 10 MOI 24 hours before injection), or with 1×10^8 cell-free Delta-24-RGD viral particles. Seven days later, brains were analyzed by immunohistochemistry for adenoviral E1A and hexon proteins (Figure 2). Viral protein expression was seen only after treated with hMSC-Delta24, indicating that effective delivery of Delta-24-RGD to gliomas requires packaging within hMSCs.

Initial localization of hMSCs-Delta24 in gliomas

We next sought to define the cellular events underlying the delivery of Delta-24-RGD by hMSCs. U87MG cells (5×10^5) were implanted into the brains of mice and after 7 days hMSCs-Delta24-AdGFP were injected into the right internal carotid artery (1×10^6 cells). Immunofluorescence staining with anti-GFP antibodies of tumors harvested immediately (within 1 hr) after injection (N=3) demonstrated gfp-labeled hMSCs within the xenografts in linear arrangements, suggesting an intravascular location (Figure 3A). Consistent with this interpretation, double immunofluorescence staining for endothelial marker PECAM1 (CD31) and GFP indicated that GFP-labeled hMSCs were located within tumor vessels (Figure 3B). To further decipher the pattern of spread of hMSCs-Delta24, xenografts were analyzed 1 to 3 days after hMSC delivery (N=3/time point). GFP-labeled hMSCs were found in clusters until day 2 (Figure 3C), after which they were dispersed through the tumor (Figure 3D). Together, these results suggest that hMSCs-Delta24 localized to gliomas via the vasculature and then migrated into the tumor parenchyma.

Spread of Delta-24-RGD from hMSCs into glioma cells

To elucidate the spread of Delta-24-RGD after arrival of hMSC-Delta24 in xenografts, we analyzed specimens treated with intravascularly delivered hMSCs-Delta24 using FITC-conjugated antibody against gfp to track hMSCs-Delta24-AdGFP, and Texas Red-conjugated anti-E1A (or anti-hexon) antibody to track Delta-24-RGD (Figure 4). Mice (n=3/ time) were implanted with U87MG xenografts and after 7 days were treated with 1×10^6 hMSC-Delta24-AdGFP (10 MOI for 24 hours). Animals were sacrifice 4, 7, and 11 days after treatment. Immunofluorescence using a FITC-conjugated antibody against GFP revealed gfp-labeled-hMSCs (green) throughout the xenografts at day 4 and fewer hMSCs at day 7. By day 11 only rare hMSCs were detected, suggesting that hMSCs-Delta24 were lysed over time. In comparison, control mice injected with hMSC-AdGFP (without Delta-24-RGD) showed hMSCs within xenografts 14 days after injection (data not shown). Immunofluorescence using Texas Red conjugated anti-E1A or Anti-hexon antibodies to track expression or Delta-24 viral proteins showed that E1A and hexon (red staining) was rare on day 4, increased on day 7, and was abundant on day 11. When merged images were analyzed after double staining with FITC-anti-GFP antibody and Texas red-Anti-E1A (or -Hexon antibody), green cells (indicative of hMSCs) were abundant on day 4, yellow cells (indicative of viral replication within hMSCs)

were evident on day 4. By day 11 red cells (indicative of U87 tumor cells expressing viral proteins) dominated the images (Figure 4A). Taken together, these findings suggest that Delta-24-RGD replicated within hMSCs, was released from lysed hMSCs, and subsequently infected U87MG-tumor cells. Hexon expression lagged behind E1A expression, as expected. Control mice injected with hMSC-GFP exhibited no evidence of adenoviral protein expression at any time (data not shown).

To quantify these results, the number of GFP-positive and E1A-positive cells were counted on at least 5 tissue sections per mouse and the cell density determined by dividing the cell count by the cross-sectional area of the xenograft (Figure 4B). E1A expression (viral replication) increased significantly over time, while GFP expression (hMSCs) decreased ($P=0.0006$, 2-way ANOVA).

To verify that these results were not unique to U87MG xenografts, similar experiments were carried out using U251-V121 glioma cell lines. In these experiments hMSCs were infected with 50 MOI Delta-24-RGD and 50 MOI Ad5/F35-CMV-GFP and injected into the carotid arteries of U251-V121-bearing mice. Similar to U87 gliomas, hMSCs-Delta24 localized to U251-V121, and supported the replication and release of Delta-24-RGD (Supplementary Figure 3A). Quantification of the result demonstrated progressive loss of hMSCs and increase in viral infection of U251-V121. However, the time course in U251-V121 was slightly accelerated compared with U87MG probably due to the infection of hMSCs with a higher amount of Delta-24-RGD (MOI 50 versus 10) (Supplementary Figure 3B).

Optimization of viral yield: *in vitro* efficacy experiments

We next sought to improve the efficiency of this approach. We administered increasing doses of GFP-labeled hMSCs to glioma-bearing mice and found that this produced increasing numbers of engrafted cells (Figure 5A). Because injection of 2×10^6 cells resulted in deaths due to respiratory failure from cells arriving in the lungs (Supplementary Figure 4), a dose of 1.5×10^6 hMSCs was used for *in vivo* efficacy experiments.

We then titrated the total amount of Delta-24-RGD produced by hMSCs at 10, 50, and 100MOI *in vitro* after 24, 48 and 72 hours, and found maximal adenoviral production at 48 hours using 100MOI (Figure 5B, *a* and *b*). Because by 72hrs many hMSCs exhibited CPE, we deduced that delivery of hMSCs 48hrs after infection with Delta-24-RGD (100 MOI) would avoid loss of virions from premature release and maximize the number of replicated virions available for tumor infection.

A Transwell assay confirmed that hMSCs release viable Delta-24-RGD that is then capable of infecting and killing U87MG cells *in vitro* (Figure 5B, *c*). Other glioma cell lines (D54, LN229, U251, U251-V121) were also found susceptible to hMSCs-Delta24 in this transwell assay (Supplementary Figure 5).

Corresponding *in vivo* experiments showed higher levels of hexon expression after 4 and 7 days in U87MG xenografts when hMSCs were incubated at 50 MOI for 24 hour and at 100 MOI for 48 hour, compared with incubating at 10 MOI for 24 hours ($n=3$ animals per group) (Figure 5C and D). Based on these experiments, hMSCs were transduced by incubating with 50MOI Delta-24-RGD for 24hrs in all *in vivo* efficacy experiments.

hMSCs-Delta24 inhibit xenograft growth and improve survival

To determine whether hMSC-Delta24 is efficacious against gliomas *in vivo*, two independent experiments were performed (Figure 6), in which mice received 1.5×10^6 hMSCs-Delta24 (50MOI \times 24 hours) via carotid artery injection 4 and 18 days after xenograft implantation. Two different luminescent U87MG cell lines (U87MG-GL in Figure 6Aa and 6Ba, and

U87MG-LucNeo in Figure 6A*b* and 6B*b*) were used. BLI showed marked differences in photon flux among the groups by 5 weeks in Experiment 1 (Figure 6C) and 3 weeks in Experiment 2 (Supplementary Figure 6A). Nonlinear regression using an exponential growth model demonstrated significant differences in the rate constants for the control and treatment arms in both experiments (Experiment 1: $P < 0.0001$, Experiment 2: $P = 0.0005$, extra sum-of-squares F-test, Supplementary Figure 6B and C). Furthermore, survival analyses demonstrated a significant improvement in median survival from 42 to 75 days in Experiment 1 and 45 to 60 days in Experiment 2 (log-rank test $P < 0.01$ for all comparisons) (Figure 6B). Survival beyond 80 days in the hMSC-Delta-24 groups was 37.5% in Experiment 1 and 36% in Experiment 2, compared with 0% in the control groups. Analysis of the brains of animals living beyond 120 days revealed no residual tumors (Supplementary Figure 7).

Discussion

Previous studies employing hMSCs carrying oncolytic adenoviruses to pulmonary metastases, soft tissue tumors, and gliomas have demonstrated limited numbers of hMSCs and adenoviral antigen-expressing cells inside the tumors (19,20,22). Efficacy of hMSC-based oncolytic viral therapy in glioma models after local delivery has not been demonstrated, and heretofore no study has attempted intravascular delivery. Thus, the results presented here elucidate for the first time the cellular events underpinning hMSC-mediated delivery of Delta-24-RGD to human gliomas and show that hMSCs-Delta24 are effective antiglioma agents after intravascular delivery.

Several investigators have raised concerns that intravascularly delivered hMSCs might not reach gliomas due to the blood brain/tumor barrier (22). However, we show that hMSCs-Delta24 localize to gliomas, probably via the tumor vasculature, and migrate into the tumor. Our findings are consistent with studies of inflammation where hMSCs participate in adhesion and transmigration cascades similar to leukocytes (29-31). Whether similar mechanisms are operant in gliomas requires further investigation.

We found that after arriving within the tumor, the number of GFP-labeled hMSCs decreased over time, while adenoviral E1A and hexon expression increased (see Figure 4). E1A and hexon expression was first found in GFP-positive hMSCs and then in non-GFP-labeled glioma cells. Together these results suggest that Delta-24-RGD replicates in hMSCs, is released through lysis of hMSCs, and then infects glioma cells. These findings are consistent with Stoff-Khalili *et al.*, who demonstrated hexon within intratumoral hMSCs carrying Ad5/3.CXCR4 after intravenous delivery to pulmonary breast metastases (20). However, their studies did not define how hMSCs reached the tumors or whether the virus infected tumor cells. Other studies did not track hMSCs and adenoviral activity simultaneously (19,21,22). Therefore, to our knowledge, our studies are the first to specifically track the progress of Delta-24-RGD from hMSC to the tumor cells.

We show that the timing of intravascular delivery of hMSCs in relation to their infection with Delta-24-RGD *ex vivo* is critical for optimizing viral yield *in vivo*. By delivering hMSCs 24-48 hours after infection with Delta-24-RGD, we were able to achieve robust tumor infection. This supports the concept that hMSCs can be harnessed as “factories” to amplify oncolytic adenoviruses (20). Viral replication appears to exploit the capacity of hMSC to self-renew, inducing inactivation of Rb as hMSCs enter S-phase. Viral titering experiments indicated that each hMSC can produce ~2,000 virions after infection with 50 MOI. We estimate that 1,000 hMSCs localize to our xenografts (data not shown). Thus, $\sim 2 \times 10^6$ virions are potentially released into the tumor after a single injection. Only intravascular doses above a threshold of 1×10^{10} adenoviral particles are capable of saturating viral clearance mechanisms to produce sufficient levels of viremia to enable tumor infection (32). In contrast, single intratumoral

injections of only 1×10^7 vp of Delta-24-RGD have been shown to retard glioma growth (33). Thus, packaging Delta-24-RGD within hMSCs is a more efficient means of infecting tumors with Delta-24-RGD than intravascular injection of free virus, and is at least as efficient as intratumoral delivery.

The dense xenograft infections elicited by hMSC-Delta24 in our animal models ultimately translated into an anti-glioma effect and prolonged animal survival. Long-term survival rates of 30-40% were achieved, and cures were demonstrated at 120 days. These results are comparable with Fueyo *et al.* who achieved a 60% long-term survival rate after administering a total of 4.5×10^8 pfu of Delta-24-RGD divided over three intratumoral injections (3,33). In comparison, we administered a total of 3×10^6 hMSCs-Delta24 divided over two intravascular injections, which resulted in an estimated total dose of $< 1 \times 10^7$ pfu Delta-24-RGD. Because hMSC-based intravascular delivery is disseminated within tumors, rather than focused at a single site as occurs with local injection, the smaller dose delivered by hMSCs was sufficient to produce a therapeutic effect comparable to intratumoral injection. Further benefit is potentially achievable by additional intravascular injections of hMSC-Delta24, which are technically difficult in small animals, but feasible in patients using endovascular techniques.

Questions remain about possible adverse effects of hMSC-Delta24. Because mice are not a natural host for adenovirus, they do not support replication of Delta-24-RGD; therefore, assessments of adverse effects of Delta-24-RGD could not be ascertained in our models. Cotton rats or Syrian hamsters, the only nonhuman species that support adenoviral replication, are needed to specifically evaluate the toxicity of Delta-24-RGD released in peripheral organs. Unfortunately, there are no syngeneic glioma lines in these animals and thus the efficacy of hMSCs-Delta24 in gliomas, the focus of this report, cannot be assessed in these animals. Nevertheless, our mouse models allowed for assessments of toxicity associated with delivering hMSCs intravascularly. Carotid injection resulted in hMSCs in the lungs, implicating pulmonary emboli as possible sources of morbidity. Recent studies also reported hMSCs in the liver for 8 months after intravenous injection (34). Given that hMSCs-Delta24 appear to be efficacious, future studies need to focus on the potential systemic toxicity of MSC-Delta24 in rat or hamster models.

Although promising, the results of our studies regarding clinical translation must be interpreted with some caution as they rely on established glioma cell lines that may not completely mimic gliomas found in situ. Although the U251 model is more infiltrative than the U87 model, both lack extensive infiltration common to gliomas. Nevertheless, these models produce significant angiogenesis, which is important for testing intravascular delivery systems such as hMSCs. In addition, much of our previously published data on Delta-24-RGD has relied on intratumoral injections of these models (2,3); therefore, they provide references for comparing intratumoral delivery of Delta-24-RGD to intravascular delivery via hMSCs. Although it may be desirable to study the effects of MSC-Delta24 in tumor models from genetically engineered mice, these approaches are not feasible because murine cells do not support adenoviral replication (see above). The recent isolation of glioma stem cells may represent an alternative model. Although these models are infiltrative, they tend to induce more limited angiogenesis, raising concerns about their application in testing intravascular delivery strategies, such as hMSCs. Nevertheless, testing of hMSCs-Delta24 in these models is currently under investigation.

Supplementary Material

Refer to Web version on PubMed Central for supplementary material.

Acknowledgments

This study was supported by grants from the Clinician Investigator Program of the Royal College of Physicians and Surgeons of Canada to R.L.Y.; the National Cancer Institute [R01 CA115729 and P50 CA 127001 to F.F.L., CA-1094551 and CA-116199 to F.C.M. and CA-55164, CA-16672, and CA-49639 to M.A.]; the M. D. Anderson Center for Targeted Therapy, The National Brain Tumor Foundation, The Elias Family Fund for Brain Tumor Research, the Gene Pennebaker Brain Cancer Fund, The Brian McCullough Research Fund, and the Run for the Roses Foundation to F.F.L.; the Susan G. Komen Breast Cancer Foundation to F.C.M.; and by the Paul and Mary Haas Chair in Genetics for M.A. We are grateful to Dr. Ayguen Sahin and Dr. Bob Carter (Harvard Medical School) for providing us with U87MG-LucNeo.

References

1. Stupp R, Mason WP, van den Bent MJ, et al. Radiotherapy plus concomitant and adjuvant temozolomide for glioblastoma. *N Engl J Med* 2005;352:987–96. [PubMed: 15758009]
2. Fueyo J, Gomez-Manzano C, Alemany R, et al. A mutant oncolytic adenovirus targeting the Rb pathway produces anti-glioma effect in vivo. *Oncogene* 2000;19:2–12. [PubMed: 10644974]
3. Fueyo J, Alemany R, Gomez-Manzano C, et al. Preclinical characterization of the antiglioma activity of a tropism-enhanced adenovirus targeted to the retinoblastoma pathway. *J Natl Cancer Inst* 2003;95:652–60. [PubMed: 12734316]
4. Krasnykh V, Dmitriev I, Mikheeva G, Miller CR, Belousova N, Curiel DT. Characterization of an adenovirus vector containing a heterologous peptide epitope in the HI loop of the fiber knob. *J Virol* 1998;72:1844–52. [PubMed: 9499035]
5. Dmitriev I, Krasnykh V, Miller CR, et al. An adenovirus vector with genetically modified fibers demonstrates expanded tropism via utilization of a coxsackievirus and adenovirus receptor-independent cell entry mechanism. *J Virol* 1998;72:9706–13. [PubMed: 9811704]
6. Chiocca EA, Abbed KM, Tatter S, et al. A phase I open-label, dose-escalation, multi-institutional trial of injection with an E1B-Attenuated adenovirus, ONYX-015, into the peritumoral region of recurrent malignant gliomas, in the adjuvant setting. *Mol Ther* 2004;10:958–66. [PubMed: 15509513]
7. Lang FF, Bruner JM, Fuller GN, et al. Phase I trial of adenovirus-mediated p53 gene therapy for recurrent glioma: biological and clinical results. *J Clin Oncol* 2003;21:2508–18. [PubMed: 12839017]
8. Kim D. Clinical research results with dl1520 (Onyx-015), a replication-selective adenovirus for the treatment of cancer: what have we learned? *Gene Ther* 2001;8:89–98. [PubMed: 11313778]
9. Alemany R, Suzuki K, Curiel DT. Blood clearance rates of adenovirus type 5 in mice. *J Gen Virol* 2000;81:2605–9. [PubMed: 11038370]
10. Lieber A, He CY, Meuse L, et al. The role of Kupffer cell activation and viral gene expression in early liver toxicity after infusion of recombinant adenovirus vectors. *J Virol* 1997;71:8798–807. [PubMed: 9343240]
11. Nakamizo A, Marini F, Amano T, et al. Human bone marrow-derived mesenchymal stem cells in the treatment of gliomas. *Cancer Res* 2005;65:3307–18. [PubMed: 15833864]
12. DiGirolamo CM, Stokes D, Colter D, Phinney DG, Class R, Prockop DJ. Propagation and senescence of human marrow stromal cells in culture: a simple colony-forming assay identifies samples with the greatest potential to propagate and differentiate. *Br J Haematol* 1999;107:275–81. [PubMed: 10583212]
13. Colter DC, Class R, DiGirolamo CM, Prockop DJ. Rapid expansion of recycling stem cells in cultures of plastic-adherent cells from human bone marrow. *Proc Natl Acad Sci U S A* 2000;97:3213–8. [PubMed: 10725391]
14. Nakamura K, Ito Y, Kawano Y, et al. Antitumor effect of genetically engineered mesenchymal stem cells in a rat glioma model. *Gene Ther* 2004;11:1155–64. [PubMed: 15141157]
15. Hall B, Dembinski J, Sasser AK, Studeny M, Andreeff M, Marini F. Mesenchymal stem cells in cancer: tumor-associated fibroblasts and cell-based delivery vehicles. *Int J Hematol* 2007;86:8–16. [PubMed: 17675260]
16. Studeny M, Marini FC, Champlin RE, Zompetta C, Fidler IJ, Andreeff M. Bone marrow-derived mesenchymal stem cells as vehicles for interferon-beta delivery into tumors. *Cancer Res* 2002;62:3603–8. [PubMed: 12097260]

17. Studeny M, Marini FC, Dembinski JL, et al. Mesenchymal stem cells: potential precursors for tumor stroma and targeted-delivery vehicles for anticancer agents. *J Natl Cancer Inst* 2004;96:1593–603. [PubMed: 15523088]
18. Klopp AH, Spaeth EL, Dembinski JL, et al. Tumor irradiation increases the recruitment of circulating mesenchymal stem cells into the tumor microenvironment. *Cancer Res* 2007;67:11687–95. [PubMed: 18089798]
19. Komarova S, Kawakami Y, Stoff-Khalili MA, Curiel DT, Pereboeva L. Mesenchymal progenitor cells as cellular vehicles for delivery of oncolytic adenoviruses. *Mol Cancer Ther* 2006;5:755–66. [PubMed: 16546991]
20. Stoff-Khalili MA, Rivera AA, Mathis JM, et al. Mesenchymal stem cells as a vehicle for targeted delivery of CRAds to lung metastases of breast carcinoma. *Breast Cancer Res Treat* 2007;105:157–67. [PubMed: 17221158]
21. Hakkarainen T, Sarkioja M, Lehenkari P, et al. Human mesenchymal stem cells lack tumor tropism but enhance the antitumor activity of oncolytic adenoviruses in orthotopic lung and breast tumors. *Hum Gene Ther* 2007;18:627–41. [PubMed: 17604566]
22. Sonabend AM, Ulasov IV, Tyler MA, Rivera AA, Mathis JM, Lesniak MS. Mesenchymal stem cells effectively deliver an oncolytic adenovirus to intracranial glioma. *Stem Cells* 2008;26:831–41. [PubMed: 18192232]
23. Rubin JB, Kung AL, Klein RS, et al. A small-molecule antagonist of CXCR4 inhibits intracranial growth of primary brain tumors. *Proc Natl Acad Sci U S A* 2003;100:13513–8. [PubMed: 14595012]
24. Szentirmai O, Baker CH, Lin N, et al. Noninvasive bioluminescence imaging of luciferase expressing intracranial U87 xenografts: correlation with magnetic resonance imaging determined tumor volume and longitudinal use in assessing tumor growth and antiangiogenic treatment effect. *Neurosurgery* 2006;58:365–72. [PubMed: 16462491]discussion -72
25. Olmsted-Davis EA, Gugala Z, Gannon FH, et al. Use of a chimeric adenovirus vector enhances BMP2 production and bone formation. *Hum Gene Ther* 2002;13:1337–47. [PubMed: 12162816]
26. Lal S, Lacroix M, Tofilon P, Fuller GN, Sawaya R, Lang FF. An implantable guide-screw system for brain tumor studies in small animals. *J Neurosurg* 2000;92:326–33. [PubMed: 10659021]
27. Fidler IJ, Schackert G, Zhang RD, Radinsky R, Fujimaki T. The biology of melanoma brain metastasis. *Cancer Metastasis Rev* 1999;18:387–400. [PubMed: 10721492]
28. Conget PA, Minguell JJ. Adenoviral-mediated gene transfer into ex vivo expanded human bone marrow mesenchymal progenitor cells. *Exp Hematol* 2000;28:382–90. [PubMed: 10781896]
29. Ruster B, Gottig S, Ludwig RJ, et al. Mesenchymal stem cells display coordinated rolling and adhesion behavior on endothelial cells. *Blood* 2006;108:3938–44. [PubMed: 16896152]
30. Segers VF, Van Riet I, Andries LJ, et al. Mesenchymal stem cell adhesion to cardiac microvascular endothelium: activators and mechanisms. *Am J Physiol Heart Circ Physiol* 2006;290:H1370–7. [PubMed: 16243916]
31. Steingen C, Brenig F, Baumgartner L, Schmidt J, Schmidt A, Bloch W. Characterization of key mechanisms in transmigration and invasion of mesenchymal stem cells. *J Mol Cell Cardiol* 2008;44:1072–84. [PubMed: 18462748]
32. Bauerschmitz GJ, Kanerva A, Wang M, et al. Evaluation of a selectively oncolytic adenovirus for local and systemic treatment of cervical cancer. *Int J Cancer* 2004;111:303–9. [PubMed: 15197787]
33. Alonso MM, Gomez-Manzano C, Bekele BN, Yung WK, Fueyo J. Adenovirus-based strategies overcome temozolomide resistance by silencing the O6-methylguanine-DNA methyltransferase promoter. *Cancer Res* 2007;67:11499–504. [PubMed: 18089777]
34. Vilalta M, Degano IR, Bago J, et al. Biodistribution, long-term survival, and safety of human adipose tissue-derived mesenchymal stem cells transplanted in nude mice by high sensitivity non-invasive bioluminescence imaging. *Stem Cells Dev* 2008;17:993–1003. [PubMed: 18537463]

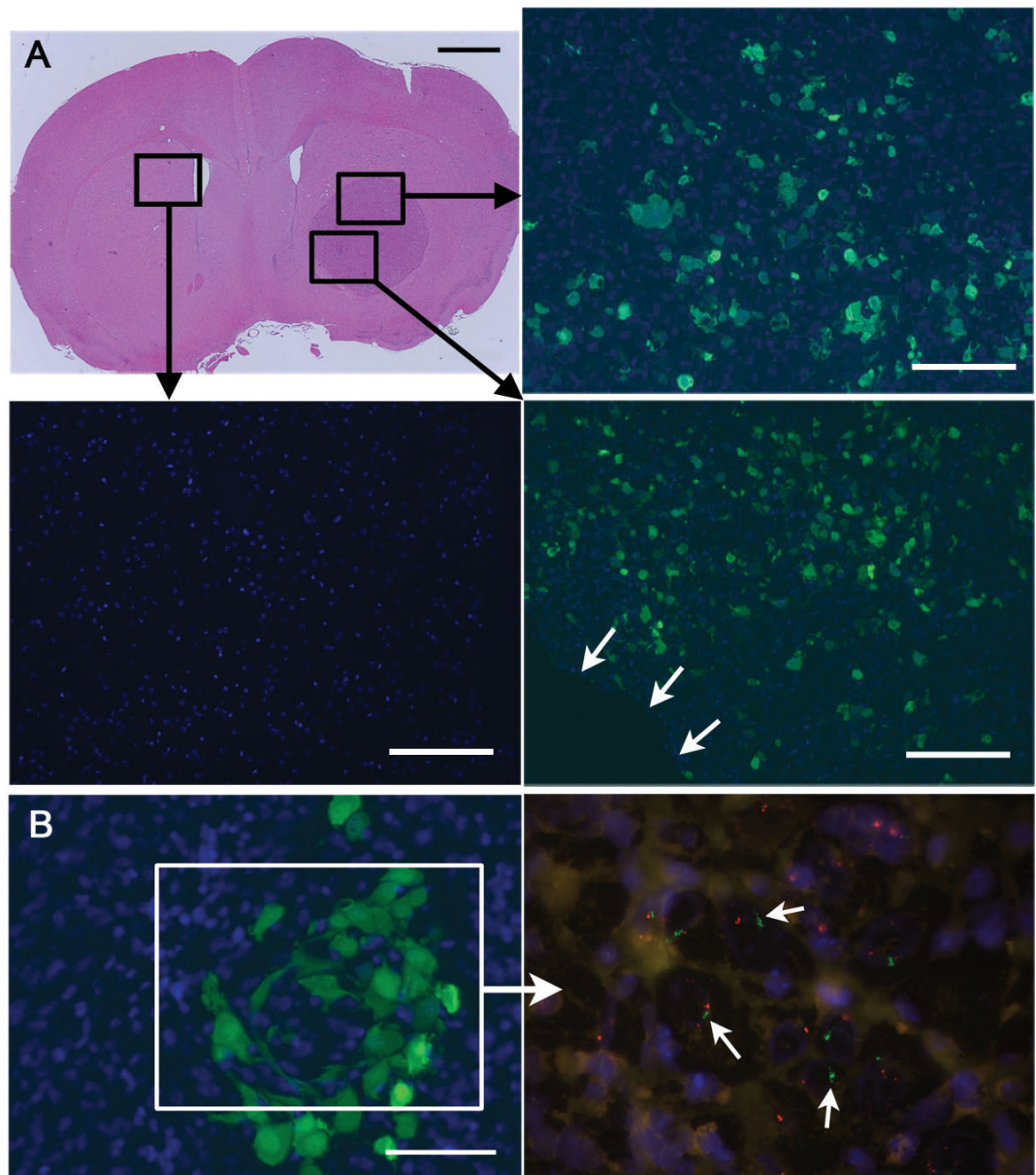


Figure 1.

A, Representative mouse implanted with U87MG in the right frontal lobe. One million GFP-labeled hMSCs were injected into the right carotid artery on day 7. The brain was extracted for histology on day 11 (scale bar 1 mm). The boxed areas were subjected to immunofluorescence using anti-GFP antibodies to reveal the distribution of hMSCs (green cells) within the xenograft. Blue = DAPI nuclear dye. **B**, A cluster of GFP-labeled hMSCs of genotype XY is seen within a U87MG xenograft of genotype XO after intracarotid delivery (scale bar 50 μ m). The boxed area shows FISH on an adjacent section to reveal Y chromosomes (green, arrows) within the area where hMSCs are present. Outside this area, only cells containing X chromosomes (red) are seen.

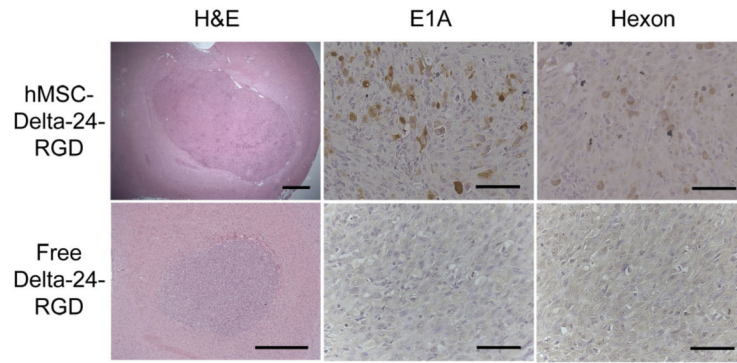


Figure 2. hMSC-Delta24 produces tumor infections while free Delta-24-RGD does not. Mice were treated as described in the text and brain sections immunostained with anti-E1A or anti-hexon antibodies. Viral E1A protein and hexon protein were seen throughout hMSCs-Delta24-treated brains (brown cytoplasmic stain) but not in controls treated with free virus. Additionally, E1A and hexon were absent in brains treated with uninfected hMSCs and phosphate-buffered saline (not shown). Scale bars 500 μ m H&E sections, and 50 μ m immunostained sections.

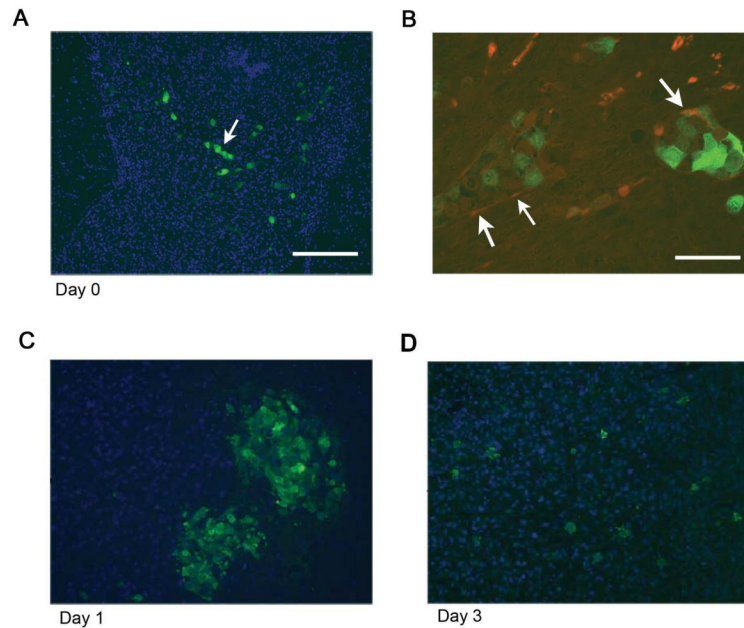


Figure 3. *A*, Brain section from a mouse sacrificed immediately after hMSC delivery demonstrating the presence of GFP-labeled hMSCs organized in linear patterns (arrows), suggesting arrival via tumor blood vessels. Scale bar 200 μ m. *B*, Section from a separate mouse stained with antibodies against endothelial marker CD31 and GFP. GFP-positive cells (green) are hMSCs and CD31 positive cells (red) are endothelial cells. Arrows show area where red endothelial cells surround green hMSCs. Scale bar 50 μ m. *C*, *D*, Mice were implanted with U87MG and then treated with hMSC-Delta24-RGD-AdGFP. Analysis of brains on days 1 and 3 by fluorescence microscopy after staining anti-GFP antibody (green) revealed hMSCs arranged in clusters on day 1 (*C*). By day 3, hMSCs had dispersed within the xenografts (*D*). Blue=DAPI.

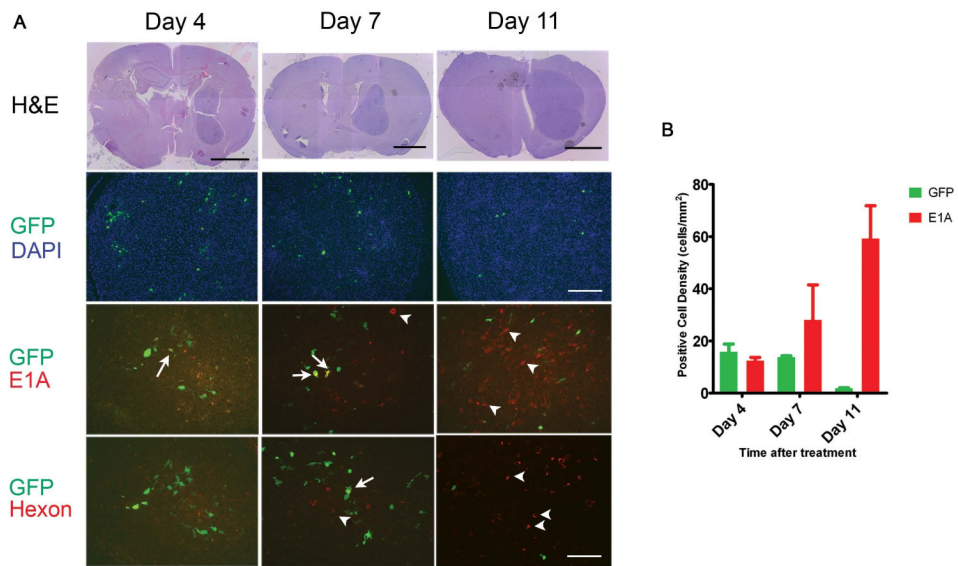
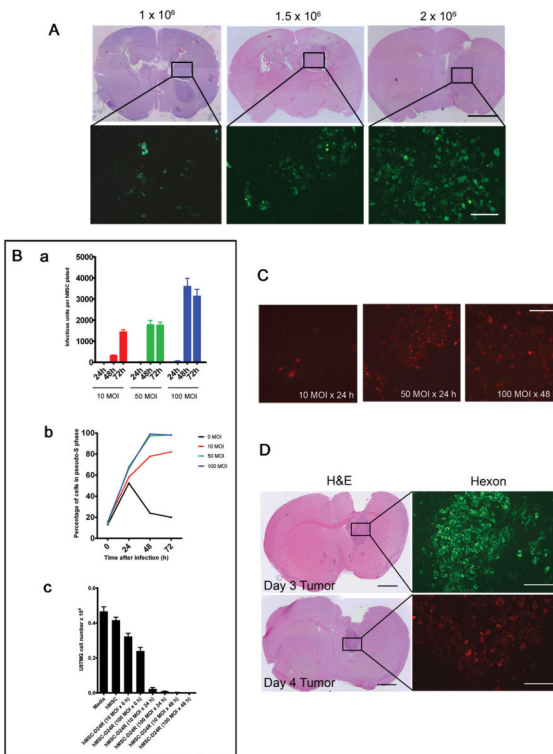


Figure 4.

A, Immunofluorescence microscopy was used to track hMSCs and Delta-24-RGD over time after intracarotid delivery to U87MG xenografts. Brains were harvested 4, 7, and 11 days after treatment. Sections were cut and stained with H&E (Upper row). Sections were double immunostained with FITC-labeled anti-GFP antibody (green) and with Texas Red-labeled anti-E1A antibody (third row, red) or Texas Red-labeled anti-hexon antibody (lowest row, red). Sections were also stained with DAPI (second row). Green cells indicate hMSCs that are not expressing viral proteins; yellow cells indicate hMSCs that are expressing viral proteins; red cells indicate U87 tumor cells expressing viral proteins. Arrows indicate examples of hMSC double-expressing GFP and E1A (yellow cells). Arrow-heads indicate examples of E1A-expressing U87MG cells (red cells). The pattern indicates progression from green to yellow to red cells, suggesting movement of virus from hMSCs to glioma cells. H&E scale bars 2mm, GFP/DAPI scale bar 200 μ m, and E1A and hexon scale bars 100 μ m. **B**, Graph showing the density of GFP-positive cells (i.e., hMSCs) and adenoviral protein-expressing cells (i.e. cells supporting viral replication) within U87MG xenografts over the course of the experiment depicted in *a*. ($p=0.0006$ for interaction, 2-way ANOVA).

**Figure 5.**

Optimization of delivery of Delta-24-RGD to U87MG xenografts via hMSCs. **A**, An increased number of delivered hMSCs correlates with an increased number of engrafted hMSCs. Mice were implanted with 5×10^5 U87MG cells in the right frontal lobe and allowed to grow for 7 days. 1.0 , 1.5 , or 2×10^6 GFP-labeled-hMSCs were injected into the carotid artery. Mice were sacrificed 4 days later. H&E scale bar 2 mm, hMSC-GFP scale bar $100 \mu\text{m}$. **B**, (a) hMSCs were infected with Delta-24-RGD at 10, 50, or 100 MOI and allowed to incubate for 24, 48, or 72 hours. Cells were collected along with media and the titer of Delta-24-RGD was measured to determine the number of infectious units released. The highest number of infectious units was obtained using 100 MOI incubated for 48 hours. Experiment performed in triplicate. (b) hMSCs were plated in serum-free media and allowed to synchronize. At 0 hours, cells were infected with Delta-24-RGD at 0, 10, 50, or 100 MOI. At the indicated time points, cell cycle analysis was performed. Results are the percentage of cells in S-phase or pseudo-S-phase. All hMSCs infected with 50 or 100 MOI exhibited evidence of viral DNA replication by 48 hours. (c) hMSCs were infected with Delta-24-RGD at the indicated MOIs, then washed and plated in the upper wells of a Transwell plate (1×10^4 cells/well). U87MG cells were plated in the bottom wells (3×10^4 cells/well) and incubate for 7 days, after which U87MG cells were counted. Killing was seen with MOIs ≥ 10 and incubation times of ≥ 24 hrs. **C**, Mice were implanted with U87MG cells and treated with hMSCs-Delta24 at the indicated MOIs and incubation times. Four days later, brains were analyzed by immunofluorescence for hexon protein expression (red cells). The 50MOI \times 24h and 100MOI \times 48h incubations produced equivalent infections. Scale bar $100 \mu\text{m}$. **D**, Mice were implanted with U87MG cells and injected IC with 1.5×10^6 hMSCs-Delta24 (50 MOI \times 24h incubation) 3 (upper) or 4 (lower) days later. On day 7 after delivery of hMSCs, xenografts were analyzed for hexon protein expression (green in top panel and red in bottom panel). H&E scale bar 1 mm, hexon scale bar $200 \mu\text{m}$.

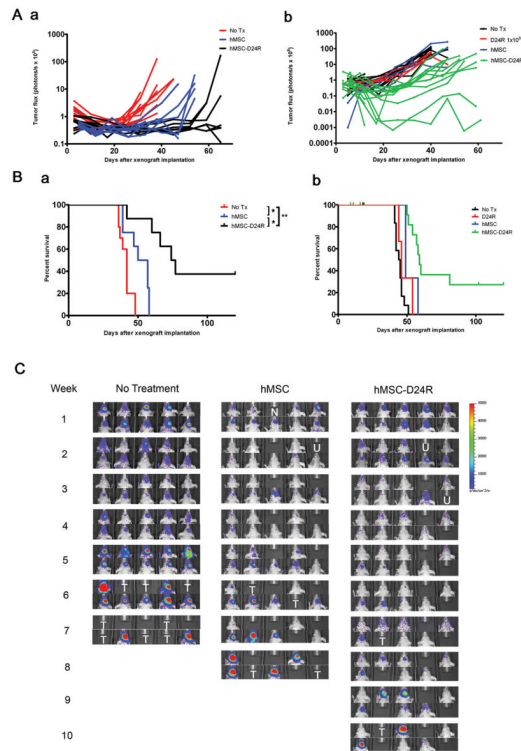


Figure 6.

A, Photon flux of xenografts over 60 days for two independent experiments in which nude mice were implanted with luminescent U87MG xenografts (U87MG-GL in *a* and U87MG-LucNeo in *b*, 5×10^5 cells). In each experiment, 10 mice were left untreated and 10-20 mice underwent two treatments with “empty” hMSCs or hMSCs-Delta24 (1.5×10^6 cells, 50MOI \times 24h incubation). Mice were imaged weekly. Total photonic flux was measured from fixed regions of interest encompassing the entire head. Each line represents efflux from a single animal. Slower growth is seen with hMSC-Delta24 treatment. **B**, Survival data corresponding to the two experiments presented in *A*. In Experiment 1 (*a*) median survival was 77 days in treated animals compared to 42 days in untreated controls and 53.5 days in animals given “empty” hMSCs. Among treated animals, 37.5% lived beyond 80 days. * $P < 0.01$ and ** $P = 0.0002$, log-rank test. In Experiment 2 (*b*), median survival was 60 days in treated animals compared to 45 days in untreated controls. 36% of animals lived beyond 80 days. *** $P < 0.0001$, log-rank test. **C**, Representative bioluminescence images over the time course of the experiment depicted in *a*. Individual mice were tracked. N, no animal. U, death unrelated to tumor. T, tumor-related death.